

# **A conceptual approach to shell buckling with emphasis on reinforced concrete shells**

Prof. Dr. Ihsan MUNGAN

Halic University

Buyukdere Cad. 101, Mecidiyekoy, 34394 Istanbul, Turkey

[imungan@halic.edu.tr](mailto:imungan@halic.edu.tr)

## **Abstract**

Author's own experimental and theoretical researches on buckling of shells of revolution are summarized with special emphasis on the conceptual approach behind them. Effect of the biaxial stress states is depicted in form of interaction diagrams. Design formulas based on these concepts and computations carried out for reinforced concrete hyperboloidal cooling tower shells allow the erection of very large and thin cooling towers which meanwhile have reached the 200m limit in height.

**Keywords:** Shell buckling, buckling stresses, cooling tower shells, ring stiffeners, effect of reinforced concrete nonlinearity.

## **1. Introduction**

No other problem of the continuum mechanics has been investigated so intensively, both theoretically and experimentally like shell buckling. Research in this field started a century ago when 1908 Lorenz [2] and 1913 Timoshenko [8] calculated for the first time the buckling stress of the cylindrical shell under axial compression. In 1915 Zoelly calculated in his dissertation the radial buckling load of the spherical shell. The interest in the theory of shell buckling was followed by its practical applications, at the beginning for the design of submarine hulls subjected externally to water pressure. After the Second World War buckling of shells became one of the most important structural problems first in aviation and afterwards for astronautics. This led to an upsurge in numerical investigations and experimental researches on shell buckling. To give an example, in 1969 there were more than 1600 publications only on the buckling of the cylindrical shell as Hutchinson and Koiter write [1]. Most of these publications were carried out considering very thin metal shells used in aviation industry and aeronautics. Such shells have a purely elastic load carrying behavior even in postbuckling region and may exhibit initial imperfections with a depth in range of 10 times or more of the shell thickness.

The interest of structural engineers and architects in shell buckling started first in the early 1950's, namely after very thin reinforced concrete shell roofs became more and more a preferred type of roofing to cover large spaces economically. Dischinger, Finsterwalder and

Rüsch had been the leaders of reinforced concrete shell roofs in Germany since the 1930'ies. Tedesco, who had worked many years with this group in the building company Dyckerhoff & Widmann continued to build shells after his emigration in the USA. Torroja in Spain, Nervi in Italy, Esquillan in France, Candela in Mexico were other masters of reinforced concrete shell roofs, whereas Zerna's mathematical shell theory submitted a very clear understanding of the General Theory of Shells during the same decade [9]. Torroja (Spain) brought the most prominent and interested theoreticians and designers of shells on September 18, 1959 together and founded the 'International Association for Shell Structures (IASS)'.

And it was again Torroja himself who was seriously concerned with the buckling problem of the very slender shell roofs built in reinforced concrete from the very beginning. As pioneer in this field Torroja conducted buckling tests on reinforced mortar models at the Central Laboratory in Madrid for such roofs, for example for the roof of the Felix und Regula Church in Zürich, Switzerland (1956) and of the Tachira Sporting Club in Venezuela (1957) shown in Fig. 1. In both cases the failure of the models was caused by buckling which, however, could not be predicted with the theory available at those years. For this reason it became urgent to study the shell buckling from the view point of structural engineering systematically.

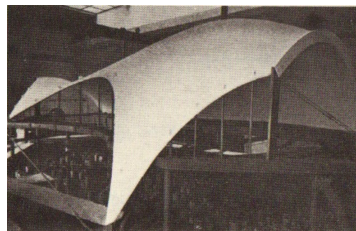


Fig. 1: Torroja's Model for the Roof of the Tachira Sporting Club in Venezuela (1957)

## **2. Author's concepts considered in his researches on shell buckling**

As explained in the foregoing chapter briefly, until the mid of the 1960'ies systematical research of the buckling problem relevant for structural engineers and architects was missing so far reinforced concrete shells were concerned. Buckling computations and tests available at those years had concentrared on the postbuckling behaviour which is of practical interest only in the case of very thin elastic shells with a radius ( $R$ ) to thickness ( $t$ ) ratio around 1000 or even larger which behave even in postbuckling range linearly elastic. In tests with such shells, although due to geometrical imperfections buckling starts always locally with a shallow single dimple, postbuckling configurations with a large number of periodical dimples require less energy dissipation than the extension and deepening of the first shallow dimple. Therefore, especially in the case of buckling tests in a rigid testing

facility with displacement control, postbuckling configurations are rather characterized through a large number of mobile periodic small dimples creating successively different buckling patterns.

In contrary to this behaviour, because of concrete's nonlinear stress-strain relationship, low tensile strength and brittleness, the theoretically possible equilibrium configurations of the postbuckling range cannot be observed in reinforced concrete shells. After the formation of the first dimple, its deepening under the existing loading leads to the cracking of concrete and failure of the shell requires less energy than formation of new dimples. Consequently, the critical or design load of the shell will be reached following the formation of the first dimple, either through crashing of concrete under compression or yielding of the reinforcement due to tension. In this way, with the first dimple coming into being, the stability problem of the reinforced concrete shell turns into an ultimate load or strength problem. This completely different postbuckling behaviour of reinforced concrete shells make a special definition of the stability or buckling as a phenomenon for these structures necessary; and for this purpose Liapunov's definition of stability in mechanics has to be adopted. According to Liapunov, the equilibrium state of a system is stable, if under the effect of a disturbance with sufficiently small magnitude, called by Liapunov 'measure', its displacements and displacement velocities, called by Liapunov 'metrics', remain sufficiently small. Such a disturbance is necessary to overcome the slight energy hump present between the unbuckled and buckled states of a shell structure as Mungan states [3].

Following Liapunov's definition, the **Introduction of a Slight Dynamic Perturbation** has been the first concept of the experimental part of author's buckling investigations in the first half of the 1960's. The second design concept of a research project directed towards buckling of reinforced concrete shells has obviously to be the **First Dimple Concept** which means the investigation of the **Local Buckling** and not necessarily of the overall buckling or postbuckling behaviour as objective. Consequently, the experimental investigations have to be carried out not in a stiff testing machine under deformation control but under **Load Control** using a sufficiently soft testing facility. In addition, as a consequence of the local buckling concept, the buckling behaviour has to be analysed and interpreted in terms of the acting stresses and not of the loading. Another reason to operate with stresses and not with loads is the fact that, depending on the support conditions, under the same loading different biaxial stress states can be activated in a shell structure. Besides, the interaction between principal stresses affects substantially the initiation of the buckling process. All these make in the case of shells necessary, to speak not of buckling stresses but of **Buckling Stress States (BSS)** which yield the so called **Interaction Diagram** for a given geometry. To be independent of the shell dimensions, the interaction diagram of each geometry has to be **Nondimensional**. Finally, each shell model has to be tested many times under different combinations of the principal stresses to eliminate the effect of the unavoidable geometrical imperfections present which may be different from one model to the other. Therefore, each model has to buckle in elastic range and recover completely after unloading to allow a series of tests under different biaxial stress states. This concept can be

expressed as the concept of **Many Tests on the Same Model**. The last concept is the **Introduction of Reduction Factors** to take account for the imperfection sensitivity for each shell geometry under corresponding uniaxial stress states. The Reduction Factors are obtained as the ratio of the uniaxial stress inducing the first dimple in the tests to the uniaxial stress obtained after the **Linear Buckling or Bifurcation Analysis** of the shell model investigated.

### 3. Results : Theory vs Tests

The geometries of the shell models tested and investigated numerically are shown at the lower right corner of Fig. 2a). The radii of curvature in the circumferential and meridional directions are indicated by the subindices 11 and 22, respectively. The radius of the cylinders (C) having zero Gaussian curvature is  $R = R_{11} = R_B = 22,5$  cm whereas the radii of the hyperbolic models (H) having negative Gaussian curvature with a radius of curvature of the meridian  $R_{22} = 63,8$  cm, are at the throat and at the boundaries  $R_T = 15,0$  cm and  $R_B = 22,5$  cm, respectively. For the spherical models (S) the radii are  $R = R_{11} = R_{22} = 37,5$  cm. For the other two shells of positive Gaussian curvature ( $E_1$ ) and ( $E_2$ ) the radii of curvature and their ratio are  $R_{22}/R_{11} = 107,2\text{cm}/26,8\text{cm} = 4$  and  $R_{22}/R_{11} = 61,0\text{cm}/30,5\text{cm} = 2$ , respectively. All shell models are  $L=60,0$  cm long, their wall thickness ( $t$ ) being 1,6 mm.

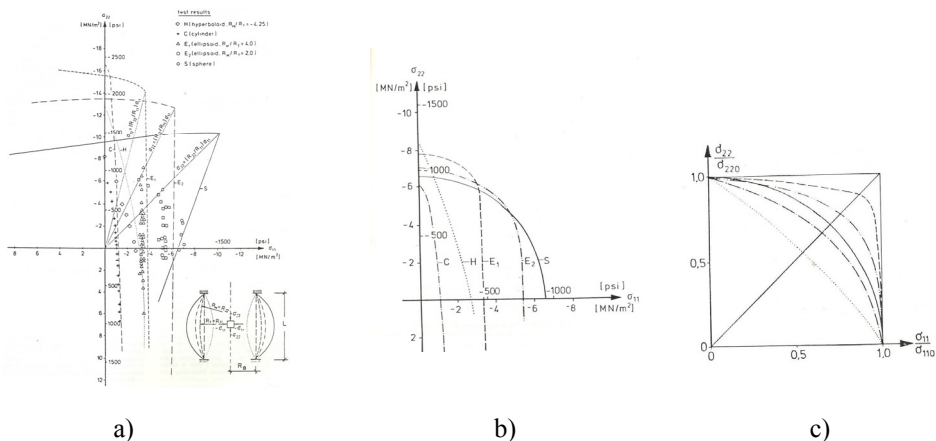


Fig.2: a) Models, Test Results, Theoretical Interaction Diagrams; b) Interaction Diagrams Fitted to the Test Results; c) Nondimensional Interaction Diagrams [3]

In Fig. 2a) taken from Mungan [3] the interaction diagrams obtained after the linear bifurcation analysis are depicted together with the test results to demonstrate the effect of the shell geometry. The interaction diagrams are for the cylindrical and hyperbolic models continuous and have the same trend as obtained in the tests. The interaction diagrams of the models having positive Gaussian curvature however, consist of two slightly curved

branches meeting at the stress state having the stress ratio equal to the ratio of the curvature radii:  $\sigma_{22} / \sigma_{11} = R_{22} / R_{11}$ . In Fig. 2b) the experimental interaction digrams fitted to the test results are depicted, whereas Fig. 2c) shows the nondimensional diagrams. The comparison of the nondimensional interaction diagrams shows that in hyperbolic shells the effect of the stress interaction is highest. They are followed by cylindrical and spherical shells in which the effect of the stress interaction is nearly the same. The effect of the stress interaction is at least for the shell models having  $R_{22} / R_{11} = 4$ .

The nondimensional interaction diagram, for the cylindrical shells can be approximated through the quadratic equation Nr. 4 of the variables  $(\sigma_{11} / \sigma_{110})$  and  $(\sigma_{22} / \sigma_{220})$  given in Fig.3 which is not symmetric with respect of these variables and contains a linear part of the variable  $(\sigma_{11} / \sigma_{110})$ . In Fig. 3 also the equations for the uniaxial buckling stresses  $\sigma_{110}$  and  $\sigma_{220}$  in circumferential and axial directions, respectively, are given. As can be seen from Eqs. 5 and 6, the uniaxial buckling stresses  $\sigma_{110}$  and  $\sigma_{220}$  are proportional to  $(t/R)^{3/2}$  and  $(t/R)$ , respectively.

For spherical shells the nondimensional interaction diagram is circular as given in Fig. 4.

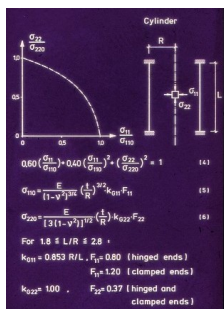


Fig. 3: Nondimensional Interaction Diagram for the Cylindrical Shells [3]

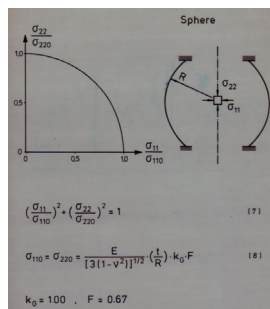


Fig. 4: Nondimensional Interaction Diagram for the Spherical Shell [3]

#### 4. Buckling of Natural Draught Cooling Tower Shells

Recently, the height of natural draught cooling towers in reinforced concrete has reached the 200m limit, whereas the base diameter is around 150m. Having a wall thickness around 20cm, cooling towers of this generation have a  $t/R$  ratio nearly equal to  $1/200$  and so are the largest and most slender reinforced concrete shells built. The shape of the shell part is a hyperboloid, i.e. has negative Gaussian curvature and therefore buckling resistance is decisive in the design of cooling towers with such large sizes considering their biaxial stress states.

In Fig. 5 the interaction diagram E obtained in tests on all models is given in full line together with dashed diagrams obtained after bifurcation analysis for the models SA, SB, CA and CB, as given by Mungan [4]. The letters S and C stand for the symmetrical and cooling tower shaped models, respectively, whereas A and B denote the boundary conditions, A stands for the fixed-in boundary without vertical displacement; in boundary condition B however, vertical displacements are allowed. Boundary condition A corresponds to the case when models are tested in a very stiff testing machine where the deepening of any local dimple is prevented. This explains the large deviation from the experimental interaction diagram allowing local buckling. On the other hand, the interaction diagram CB calculated for the cooling tower shaped models with the boundary condition allowing vertical displacement has the best agreement with the test results.

The nondimensional interaction diagram obtained in tests on hyperboloidal shells can be approximated through the quadratic equation Nr.1 of Fig. 6. This equation is symmetric with respect of the the variables  $(\sigma_{11} / \sigma_{110})$  and  $(\sigma_{22} / \sigma_{220})$ . Besides, according to Eqs. 2 and 3,  $(t/R)$  which is the measure of the shell slenderness has the same effect on the uniaxial buckling stresses  $\sigma_{110}$  and  $\sigma_{220}$  in circumferential and meridional directions, respectively. The geometry factor  $k_{G22}$  for the uniaxial buckling stress in meridional direction is 8,4 times bigger than that for the circumferential direction  $k_{G11}$ . The reduction factor  $F_{22} = 0,62$  for the buckling stress in the meridional direction means a higher reduction at the same time; but at the end following relation comes out:  $\sigma_{220} = 6,05 \sigma_{110}$ . This means that the buckling resistance is lower against circumferential stresses. Therefore, to increase the buckling resistance of cooling tower shells the arrangement of stiffening rings becomes the most efficient measure.

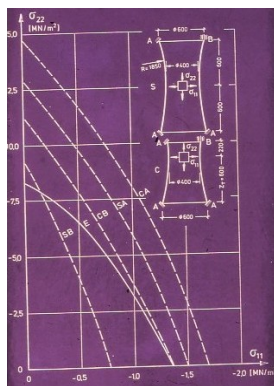


Fig. 5: Interaction Diagrams for the Models Tested [4]

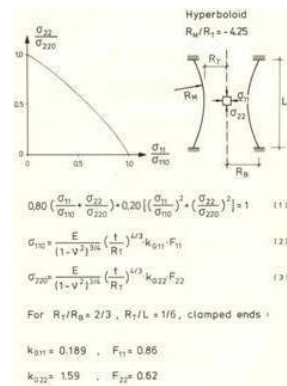


Fig. 6: Nondimensional Interaction Diagram for the Hyperboloidal Shells [4]

## 5. Numerical Investigations on the Effect of Stiffening Rings

Numerical parameter studies and buckling tests on ring stiffened cooling tower shell models have provided following parameters to be governing with respect to the efficiency of stiffening rings on the buckling resistance:

- Size of the stiffening rings,
- Location of the stiffening rings,
- Number of the stiffening rings.

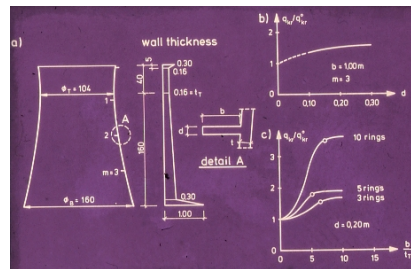


Fig. 7: Size Effect of the Ring Stiffeners [4]

The effect of the thickness ( $d$ ) and the width ( $b$ ) of ring stiffeners on buckling due to uniform external lateral pressure is shown in Fig. 7. Curve b) in this figure demonstrates the rather slight effect of the ring thickness on the buckling pressure if it is increased twofold or threefold for the cooling tower given in graph a). In contrary to this, the effect of the depth or width of the rings is much more pronounced as shown in curves c) which is obtained in the case of equidistant arrangement of three, five or ten rings along the meridian. According to these curves a width equal to at least six times of the local shell thickness provides the optimal augmentation, as given in Mungan and Lehmkamper [4].

The most effective location for the first stiffening ring is the throat where the first dimple shapes. The locations for the successive rings are obtained each time by placing the new ring at the location where the previous buckling configuration has its peak. For a number of rings more than five the equidistant positioning is efficient as well [5].

## 6. Experimental Investigations on the Effect of Stiffening Rings

To check the results obtained numerically, hyperboloidal models were tested by the author first without rings and than after stiffening by means of five, nine or 19 rings at equidistant locations [6]. The width and thickness of the rings were 7.5 mm and 2.0 mm, respectively, giving a width to shell thickness ratio of about 6 which turned out to be optimal according to the computations. Interaction diagrams E for loads as obtained experimentally and T calculated applying the bifurcation theory are given at the left side of Fig. 8. The theoretical interaction diagram of the shell stiffened by means of 19 rings,  $T_{19}$  is omitted in the figure, because in this case the numerical results depend substantially on the assumption of global



or local loss of stability; furthermore, in the case of local instability on where the first dimple is assumed to develop.

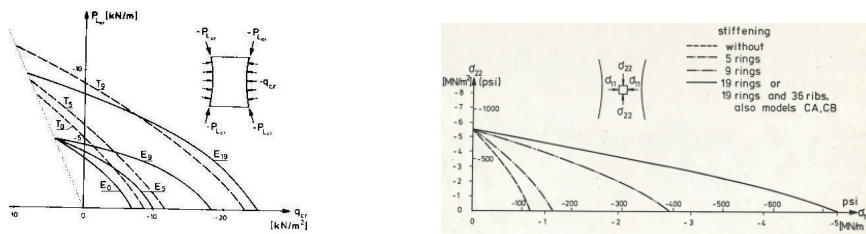


Fig. 8: Ring Stiffened Models Tested and the Interaction Diagrams Obtained [6].

If the four experimental load interaction diagrams are considered, it is interesting to notice that  $E_0$ ,  $E_5$  and  $E_9$  intersect in one point corresponding to the combination of the axial compression with internal radial pressure. Under the same load combination however, in the case of the models stiffened by means of 19 rings the critical axial load  $P_{Lcr}$  is twice as high. On the other hand, if the interaction diagrams are depicted in terms of the stresses as shown in the right part of Fig. 8, in all cases the same uniaxial buckling stress in the meridional direction  $\sigma_{220}$  is obtained. With increasing number of the stiffening rings the first dimple observed in the tests shifts from the throat to the upper or lower part of the model where the radius of rotation is greater. Consequently, at these locations for the same external pressure the buckling stress in the circumferential direction  $\sigma_{110}$  increases whereas  $\sigma_{220}$  decreases. As the curves at the right part of Fig. 8 show,  $\sigma_{110}$  increases 1.40, 3.34 or even 6.30 times after stiffening of the same model by means of five, nine or 19 rings, respectively, whereas the value of  $\sigma_{220}$  is not affected by the ring stiffening. The equation of all four nondimensional interaction diagrams in terms of  $(\sigma_{11} / \sigma_{110})$  and  $(\sigma_{22} / \sigma_{220})$  is the same as Eq. (1) in Fig. 6.

The final stiffening effect of the number of rings is obtained by means of numerical analysis on a 165m high cooling tower shell with 83,5m and 150m diameters at the throat and base, respectively. The wall thickness of the shell was determined considering the lowest local buckling safety factor  $\gamma_B = 5$  without any ring stiffening. Arranging rings of different number in most effective positions buckling safety factors higher than 5 are obtained. The augmentation of the buckling safety factor is depicted in Fig. 9 as given in Mungan [4]. For the cooling tower shell investigated the diagram has its highest inclination at a number of rings equal to four, which means four rings are to be considered as optimal.



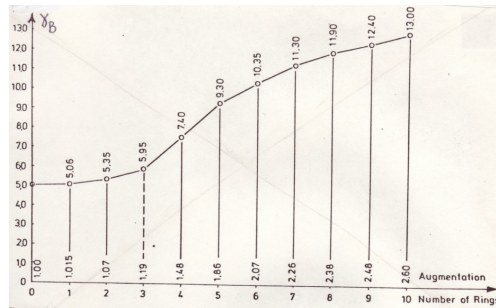


Fig. 9: Number of Stiffening Rings vs. Augmentation of the Buckling Safety Factor [4].

## 7. Investigation of the Effect of Nonaxisymmetric Loading: Wind Tunnel Tests

Fig.10 shows three out of two large series of wind tunnel tests carried out by Ruhwedel on models having alternately a circle or hyperbola as meridian to check the validity of the results obtained under axisymmetric loading and circular meridian also for models having a hyperbola as meridian and subjected to wind action which is nonaxisymmetric [7].



Fig. 10: Models Without and With an Upper Edge Ring ; Model With Internal Suction [7].

The wind tunnel tests yielded following results:

- An upper edge ring does not change the magnitude of the critical wind load or the stress states leading to local buckling. Only the buckling configuration changes as the first two photographs show. This behaviour is in favour of the approach based on the local buckling concept.
- In the load case with internal suction, even without an upper edge ring the buckling configuration is similar to the case with an upper ring as the two photographs at the right show. Again the stress state initiating the buckling fit into the interaction diagram obtained in tests under axisymmetric stress states.

- Either circular as in the tests under axisymmetric loading or a hyperbola, there is no influence of the geometry of the meridional curve on the buckling stress states in terms of the geometric parameters of the shell, namely the ratio of the radii at the throat and at the base ( $R_T / R_B$ ) and the ratio of the shell radius at the throat to the height of the throat from the base ( $R_T / Z_T$ ).
- Variable wall thickness has no influence on the interaction diagram [7].
- The uniaxial buckling stresses  $\sigma_{110}$  and  $\sigma_{220}$  in circumferential and meridional directions, respectively, obtained in the wind tunnel tests are 25% less than those obtained in tests under axisymmetric loading. The bending moments present from the very beginning cause this difference. There are two causes for these bending moments resulting from the initial imperfections of the models. First cause is the rather small wall thickness of the wind tunnel models which is between 0,78 mm and 1,05 mm and as such less than the wall thickness 1,20 mm to 1,93 mm of the models tested under axisymmetric stress states. In addition, the modulus of elasticity of the Polyurethan-Elastomer material, called Vulkollan, used in models tested in wind tunnel is 40kN/cm<sup>2</sup>, whereas the modulus of elasticity of epoxy resin, called Araldite, used in tests under axisymmetric loading is with 345kN/cm<sup>2</sup> nearly 9 times higher. Because of these two reasons the models tested in wind tunnel are much softer than those tested under axisymmetric loading and therefore are also more susceptible to initial imperfections induced during their production or installation. Larger imperfections make lower correction factors necessary.
- So far the effect of the intermediate stiffening rings is concerned, there is no difference between the two test series [7].

## 8. Investigation of the Effect of the Nonlinear Behaviour and Cracking of Reinforced Concrete

Because of two effects the BSS-Approach developed may need a modification when applied to the buckling of reinforced concrete cooling tower shells. These two effects are the nonlinearity of concrete under compression and its cracking under tension which finally causes yielding of the reinforcement. If the compressive stresses in concrete are so high that the curved part of concrete's stress-strain diagram is decisive, then the stress state dependent local tangent moduli of concrete have to be considered in the buckling analysis. Consequently, with increasing Load Factor (LF) the local buckling safety factor ( $\gamma_{LB}$ ) decreases more than that computed assuming a linear elastic material behaviour. The curve depicted in Fig. 11 demonstrates this fact. Up to load factor 3 the local buckling safety factor is overall bigger than 1.0. However, at LF = 4 the region between 15m and 120m from the base becomes unstable ( $\gamma_{LB} < 1.0$ ). At LF = 5 the whole cooling tower is unstable and the destruction due to compression starts in the section at the elevation 15m from the base where the thickening of the lower edge member begins, as in Zerna *et al.* [10].

On the other hand, in cooling tower shells subjected to wind action there are some areas where the resultant action from self weight and wind loading is a tensile membrane force.

In contrast to the areas compressed in both directions and which are therefore critical with respect of buckling or crushing of concrete under compression, no danger of local buckling exists in the zones under tension. However, in such zones the strength of the section against tension, i.e. yielding of the reinforcement is the problem which is again a local phenomenon. Because buckling design yields the wall thickness required and in this way also the self weight of the cooling tower shell, there is an interaction between both problems. Increasing the safety factor prescribed against local buckling results in thicker shell wall, higher prestressing through self weight, lower resultant tensile membrane forces and, consequently, a higher ultimate load factor under wind load.

In order to get transparency in the rather complicated interaction of both failure mechanisms, cooling towers having three different geometries are investigated with respect of both buckling resistance and tensile strength. The correlation between the design buckling safety factor ( $\gamma_B$ ) and the ultimate wind load factor ( $\gamma_{UW}$ ) is depicted in Fig. 12. With increasing cooling tower diameter for the same height,  $\gamma_{UW}$  may be greater than  $\gamma_B$ , which means buckling precedes the tensile failure due to wind, as explained in Mungan [4].

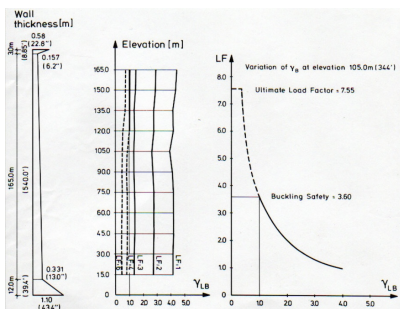


Fig. 11: Effect of the Nonlinear Behaviour of Concrete on the Buckling Safety [10]

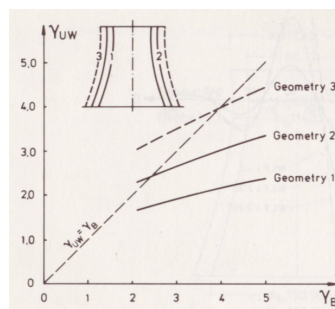


Fig. 12: Ultimate Load Factor for wind vs. Design Buckling Safety [10]

## 9. Conclusions and Acknowledgements

The concepts on which the present approach of buckling stress states (BSS) is based proved to be very efficient in buckling design of shells as demonstrated on natural draught cooling tower shells. The approach can also be extended on shell roofs under support conditions preventing inextensional deformations. As further numerical investigations has shown, even in the case of cooling tower shells such deformations which can be induced through support settlements may have a very detrimental effect on the local and consequently on the global buckling resistance of the shell structure, as explained in Mungan [4].

The tests and numerical investigations presented in this paper had been carried out in Prof. Wolfgang Zerna's Lehrstuhl I (Chair for Concrete Structures) at Ruhr University Bochum

between 1972 and 1985. Prof. Zerna (1916 -2005) was one the founders of the International Association for Shell Structures (IASS) and had contributed substantially to the theory and design of shell structures through his works. From 1972 to 1985 Prof. Zerna's shell research group had been guided by the author of this paper. The extensive numerical results referred partly in this paper were calculated by many research assistants for their Doctoral Theses. The research projects were financed mainly by the DFG (German Research Association) and by the Ministry for Science and Research of the State North Rhine Westphalia, Federal Republic of Germany.

## 10. References

- [1] Hutchinson, J. W. and Koiter, W. T., Postbuckling Theory, *Applied Mechanics Reviews*, 1970; **23**; 795-806.
- [2] Lorenz, R., Achsensymmetrische Verzerrungen in dünnwandigen Hohl zylindern, *Zeitschrift des Vereins deutscher Ingenieure (VDI)*, 1908; **52**; 1706.
- [3] Mungan, I., Some Observations on Shell Buckling', *Bulletin of the International Association for Shell and Spatial Structures*, 1983; **81**; 3-11.
- [4] Mungan, I., Wind-Buckling Approach for R/C Cooling Towers, *Civil Engineering Practice I/ Structures*, P.N. Chermisinoff, N.P. Chermisinoff and S.L. Cheng Editors, Technomic Publishing Co. Inc., 1987, 627-661.
- [5] Mungan, I. and Lehmkämper, O., Buckling of Stiffened Hyperboloidal Cooling Towers, *Journal of the Structural Division, ASCE*, 1979; **105**; 1999-2007.
- [6] Mungan, I., Buckling Stresses of Stiffened Hyperboloidal Shells, *Journal of the Structural Division, ASCE*, 1979; **105**, 1589-1604.
- [7] Ruhwedel, J., *Experimentelle Beuluntersuchungen von Kühlturmschalen unter Windbelastung*, Institut für Konstruktiven Ingenieurbau, Ruhr-Universität Bochum, Technical Reports Nr. 86-6, 1986.
- [8] Timoshenko, St. (1910): 'Einige Stabilitätsprobleme aus der Elastizitätstheorie', *Zeitschrift für Mathematik und Physik*, 1910; **58**; S. 360.
- [9] Zerna, W., A New Formulation of the Theory of Elastic Shells, *Bulletin of the International Association for Shell and Spatial Structures*, 1969; **36**; 61-76.
- [10] Zerna, W., Mungan, I and Steffen, W., Wind-Buckling Approach for RC Cooling Towers, *Journal of Engineering Mechanics, ASCE*, 1983; **109**; 836-848.